

This discussion paper is/has been under review for the journal Atmospheric Chemistry and Physics (ACP). Please refer to the corresponding final paper in ACP if available.

# Investigating the use of secondary organic aerosol as seed particles in simulation chamber experiments

J. F. Hamilton<sup>1</sup>, M. Rami Alfarra<sup>2,3</sup>, K. P. Wyche<sup>4</sup>, M. W. Ward<sup>1</sup>, A. C. Lewis<sup>1</sup>, G. B. McFiggans<sup>3</sup>, N. Good<sup>3,\*</sup>, P. S. Monks<sup>4</sup>, T. Carr<sup>4</sup>, I. R. White<sup>4</sup>, and R. P. Purvis<sup>1</sup>

<sup>1</sup>Department of Chemistry, University of York, Heslington, York, YO10 5DD, UK

<sup>2</sup>National Centre for Atmospheric Science (NCAS), School of Earth, Atmospheric and Environmental Sciences, University of Manchester, Manchester, M13 9PL, UK

<sup>3</sup>Centre for Atmospheric Science, School of Earth, Atmospheric and Environmental Sciences, University of Manchester, Manchester, M13 9PL, UK

<sup>4</sup>Atmospheric Chemistry Group, Department of Chemistry, University of Leicester, Leicester, LE1 7RH, UK

## Investigating the use of secondary organic aerosol

J. F. Hamilton et al.

Title Page

Abstract

Introduction

Conclusions

References

Tables

Figures

⏪

⏩

◀

▶

Back

Close

Full Screen / Esc

Printer-friendly Version

Interactive Discussion



\*now at: Laboratoire de Météorologie Physique, Blaise Pascal Univ., Clermont-Ferrand, 63000, France

Received: 13 October 2010 – Accepted: 20 October 2010 – Published: 27 October 2010

Correspondence to: J. F. Hamilton (jfh2@york.ac.uk)

Published by Copernicus Publications on behalf of the European Geosciences Union.

ACPD

10, 25117–25151, 2010

## Investigating the use of secondary organic aerosol

J. F. Hamilton et al.

Title Page

Abstract

Introduction

Conclusions

References

Tables

Figures

◀

▶

◀

▶

Back

Close

Full Screen / Esc

Printer-friendly Version

Interactive Discussion



## Abstract

The use of  $\beta$ -caryophyllene secondary organic aerosol particles as seeds for smog chamber simulations has been investigated. A series of experiments were carried out in the Manchester photochemical chamber as part of the Aerosol Coupling in the Earth System (ACES) project to study the effect of seed particles on the formation of secondary organic aerosol (SOA) from limonene photo-oxidation. Rather than use a conventional seed aerosol containing ammonium sulphate or diesel particles, a method was developed to use in situ chamber generated seed particles from  $\beta$ -caryophyllene photo-oxidation, which were then diluted to a desired mass loading (in this case 4–13  $\mu\text{g m}^{-3}$ ). Limonene was then introduced into the chamber and oxidised, with the formation of SOA seen as a growth in the size of oxidised organic seed particles from 150 to 325 nm mean diameter. The effect of the partitioning of limonene oxidation products onto the seed aerosol was assessed using aerosol mass spectrometry during the experiment and the percentage of  $m/z$  44, an indicator of degree of oxidation, increased from around 5 to 8%. The hygroscopicity of the aerosol also changed, with the growth factor for 200 nm particles increasing from less than 1.05 to 1.25 at 90% RH. The detailed chemical composition of the limonene SOA could be extracted from the complex  $\beta$ -caryophyllene matrix using two-dimensional gas chromatography (GC $\times$ GC) and liquid chromatography coupled to mass spectrometry. High resolution Fourier Transform Ion Cyclotron Resonance Mass Spectrometry (FTICR-MS) was used to determine exact molecular formulae of the seed and the limonene modified aerosol. The average O:C ratio was seen to increase from 0.32 to 0.37 after limonene oxidation products had condensed onto the organic seed.

## 1 Introduction

Atmospheric aerosols affect the climate through both direct and indirect radiative processes, however there remain significant uncertainties in the magnitude and variability

ACPD

10, 25117–25151, 2010

## Investigating the use of secondary organic aerosol

J. F. Hamilton et al.

Title Page

Abstract

Introduction

Conclusions

References

Tables

Figures

◀

▶

◀

▶

Back

Close

Full Screen / Esc

Printer-friendly Version

Interactive Discussion



of effects, arising from limited knowledge on sources, composition, properties, and the mechanisms of their formation (Fuzzi et al., 2006). The gas phase oxidation of biogenic compounds in the atmosphere can result in the formation of lower volatility species which can form biogenic secondary organic aerosol (BSOA), one of the most uncertain factors in the global radiation budget (Intergovernmental Panel for Climate Change, 2007). Recent modelling studies of atmospheric aerosols using explicit chemical mechanisms based on results from simulation chambers experiments have shown a significant under-prediction of secondary organic aerosol formation (SOA) when compared to measurements (Capes et al., 2009; Volkamer et al., 2006). One explanation for this effect is a lack of background particles in traditional smog chamber experiments. In chambers where particle formation occurs by nucleation, there is an induction time for SOA formation as condensable products must exceed saturation vapour pressures. Whilst organic nucleation is not widely observed in the real atmosphere, it can be considered more reasonable for oxidised VOC products to condense on to pre-existing aerosols. Better simulation in chamber experiments can therefore be achieved by including background or “seed” particles for oxidised products to partition onto.

It is a criterion of absorptive partitioning theory that all condensed components are miscible across the whole concentration range, and thus the greatest amount of interaction is likely to take place when seed particles have similar properties as the compounds condensing onto them. Historically, most chamber experiments have used inorganic aqueous solutions of ammonium sulphate or sulphuric acid as seed aerosols to study SOA formation (Hallquist et al., 2009). These studies have shown the formation of organosulphate species in monoterpene and isoprene SOA, which have also been seen in ambient samples (Iinuma et al., 2007; Liggio and Li, 2006; Surratt et al., 2007). Volkamer et al. (2009), found that the yield of SOA from acetylene photo-oxidation, where the main product is glyoxal, strongly depends on the chemical composition of the seed particles. In this case, use of an ammonium sulphate seed led to one of the lowest SOA yields. However, the yield was significantly increased by the addition

## Investigating the use of secondary organic aerosol

J. F. Hamilton et al.

Title Page

Abstract

Introduction

Conclusions

References

Tables

Figures

◀

▶

◀

▶

Back

Close

Full Screen / Esc

Printer-friendly Version

Interactive Discussion



of fulvic acid to the ammonium sulphate. Jang et al., 2003 used seed particles from diesel engine exhaust in chamber studies to mimic primary organic aerosol. However, diesel and fulvic acid are made up of thousands of compounds and identifying SOA components arising from a known precursor in such a complex matrix is extremely difficult. In both cases there is a disparity between the chemical properties of the seed and the oxidised organic compounds partitioning to form SOA. In the atmosphere most organic aerosol (OA) is oxidised, even in urban areas (Jimenez et al., 2009; Zhang et al., 2007). Thus, a better seed particle to simulate many environments would be an oxidised organic aerosol (OOA). There are a number of difficulties involved with using OOA as a seed. Firstly, which organic compound is most suitable? Previous studies have used dioctylphthalate (Song et al., 2007) and highly oxidised organic acids (Corrigan et al., 2008) as a surrogate of SOA, but these are single compounds, rather than the range of molecular weights and functionalities seen in the atmosphere. Oxidised compounds are also generally difficult to work with and stick to surfaces.

A more appropriate seed for investigating the partitioning of a wide range of semi-volatile OVOCs would be SOA itself. Dommen et al. (2009) used  $\alpha$ -pinene SOA as a seed aerosol for isoprene SOA although the isoprene was  $^{13}\text{C}$  labelled to allow the seed to be differentiated. This method required the use of plants to fix  $^{13}\text{CO}_2$ , which then emitted labelled isoprene and thus is limited to this particular VOC. Here we present the use of sesquiterpene SOA, formed from  $\beta$ -caryophyllene photo-oxidation, as a seed particle for simulation chamber experiments. Within this work,  $\beta$ -caryophyllene SOA seed has been used to study the generation of SOA from limonene photo-oxidation.  $\beta$ -Caryophyllene reacts rapidly with hydroxyl radicals and ozone resulting in almost immediate nucleation owing to the high molecular weight and low volatility of its first generation oxidation products. The chamber was subsequently diluted to obtain a low particle concentration and remove the majority of the gas phase products. The VOC to be studied, in this case limonene, was then introduced into the chamber and oxidised. The gas phase loss of limonene and the formation of its oxidation products were followed by Chemical Ionisation Reaction Time of Flight Mass

## Investigating the use of secondary organic aerosol

J. F. Hamilton et al.

Title Page

Abstract

Introduction

Conclusions

References

Tables

Figures

◀

▶

◀

▶

Back

Close

Full Screen / Esc

Printer-friendly Version

Interactive Discussion



Spectrometry (CIR-TOF-MS). The partitioning of limonene oxidation products to the seed was followed by monitoring the shift in the particle size distribution. The change in bulk chemical composition was analysed in real time using Aerosol Mass Spectrometry. The difference in the detailed chemical composition between the seed and the limonene SOA was analysed offline using Comprehensive Two-dimensional Gas Chromatography Time-of-Flight Mass Spectrometry (GC×GC-TOF/MS), Liquid Chromatography Ion Trap Mass Spectrometry (LC-MS<sup>n</sup>) and Fourier Transform Ion Cyclotron Resonance Mass Spectrometry (FTICR-MS).

## 2 Experimental

### 2.1 Chamber

The Manchester photochemical chamber is an 18 m<sup>3</sup> (3 m (H)×3 m (L)×2 m (W)) FEP Teflon bag mounted on three rectangular aluminium frames. The central rigid rectangular frame is fixed, with the upper and lower frames free to move vertically causing the bag to expand and collapse as sample air is introduced and extracted. A bank of halogen lamps and a 6 kW Xenon arc lamp are mounted on the enclosure housing the bag which is coated with reflective “space blanket” serving to render the enclosure as an integrating sphere, maximising the irradiance in the bag and ensuring even illumination. The combination of illumination has been tuned and evaluated to replicate the atmospheric actinic spectrum. Air conditioning between the enclosure and the bag removes additional unwanted heat generated by the lamps. The air charge in the bag is dried and filtered for gaseous impurities and particles using a combination of Purafil, charcoal and HEPA filters, prior to humidification with ultrapure deionised water.

Parent VOCs are introduced into the chamber through injection into a heated glass bulb fed with a flow of filtered nitrogen. NO<sub>x</sub> levels are controlled by injection from a cylinder into the charge line and a high capacity O<sub>3</sub> generator was employed to control initial O<sub>3</sub> concentrations as well as serving as a cleaning agent during flushing between

## Investigating the use of secondary organic aerosol

J. F. Hamilton et al.

Title Page

Abstract

Introduction

Conclusions

References

Tables

Figures



Back

Close

Full Screen / Esc

Printer-friendly Version

Interactive Discussion



experiments. Cycling between experiments is facilitated by full computer control as is the monitoring of key chamber conditions (e.g. temperature and relative humidity). Automatic fill/flush cycling to clean the chamber before and after each experiment with  $3\text{ m}^3\text{ min}^{-1}$  flow of scrubbed, dried, rehumidified (and optionally ozonised) air is achieved by control of electro-pneumatic valves. Each cycle takes approximately 12 min and cleaning is normally achieved after 5 or 6 cycles. Coupling morning and evening cycling with overnight soaking at ppm levels of  $\text{O}_3$ , allows experiments to be carried out on subsequent days. Longer experiments are possible on 2-day cycles. Relative humidity (RH) and Temperature ( $T$ ) are measured at several points throughout the chamber (by dewpoint hygrometer and a series of thermocouples and resistance probes, respectively) and are controlled by diverting air through the inlet humidification circuit and by controlling the air conditioning setpoint, respectively.

## 2.2 Experimental methodology

The secondary organic aerosol seed was generated from  $\beta$ -caryophyllene in the presence of  $\text{NO}_x$  (Initial  $\text{VOC}:\text{NO}_x \sim 1-2$ ) using a conventional nucleation and growth experiment. The experimental details are summarised in Table 1. Approximately 98–99% of the precursor  $\beta$ -caryophyllene had reacted after about 3 h. This was verified using the CIR-TOF-MS. After this time, chamber lights were turned off, and a fraction of the chamber content was flushed out and replaced by clean air. This resulted in dilution of the seed concentration down to approximately 4 to  $13\ \mu\text{g m}^{-3}$ , depending on the experiment, and also the dilution of the gas phase reactants. During the dilution phase, limonene was injected into the chamber and, if required, the  $\text{NO}_x$  level was adjusted to keep the  $\text{VOC}:\text{NO}_x$  ratio at around 2 (a fixed ratio was favourable to enable comparisons between experiments). Following this flush/refill phase, chamber lights were turned back on again to allow for the photooxidation of limonene.

Filters were collected in a specially constructed holder, positioned in the chamber vent line. Aerosol samples were collected onto 47 mm quartz fibre filters (Whatman) at a flow rate of  $3\text{ m}^3\text{ min}^{-1}$ . Filters were collected during the dilution stage to obtain a  $\beta$ -

### Investigating the use of secondary organic aerosol

J. F. Hamilton et al.

Title Page

Abstract

Introduction

Conclusions

References

Tables

Figures

◀

▶

◀

▶

Back

Close

Full Screen / Esc

Printer-friendly Version

Interactive Discussion



caryophyllene seed sample, which was used as a background for the limonene SOA. Limonene SOA + seed samples were collected at the end of the experiment. After sampling, filters were immediately placed in pre-cleaned glass vials and stored below  $-20^{\circ}\text{C}$  until analysis.

Experiments were carried out at  $25^{\circ}\text{C}$  and nominal relative humidity of 70%. Chamber humidity was controlled using vapour from heated ultra pure water (Purelab Ultra System, Elga). Known amounts of  $\beta$ -caryophyllene ( $\text{C}_{15}\text{H}_{24}$ , Sigma Aldrich) and limonene ( $\text{C}_{10}\text{H}_{16}$ , Fluka  $\geq 99.0\%$ ) were evaporated from a heated glass bulb and continuously flushed into the chamber using a flow of nitrogen.  $\text{NO}_2$  was introduced into the chamber from a cylinder containing 10%  $\text{NO}_2$  in nitrogen.

### 2.3 Gas phase

$\text{NO}$  and  $\text{NO}_2$  mixing ratios were measured using a chemiluminescence detector (Model 42i, Thermo Scientific, MA, USA). Ozone was measured using a UV photometric gas analyser (Model 49C, Thermo Scientific, MA, USA). The gas phase organic compounds within the chamber were measured using Chemical Ionisation Reaction Time-of-Flight Mass Spectrometry (CIR-TOF-MS). This technique has been described in detail elsewhere (Blake et al., 2004; Wyche et al., 2007), hence here it is only described in brief alongside experiment specific details.

The CIR-TOF-MS instrument comprises a bespoke, temperature controlled ( $40^{\circ}\text{C}\pm 0.5$ ) radioactive ( $^{241}\text{Am}$ ) ion source/drift cell assembly, coupled to an orthogonal time-of-flight mass spectrometer equipped with a reflectron array (Kore Technology Ltd, Ely, UK). During these experiments, proton transfer reaction ionisation was employed as the chemical ionisation technique, utilising hydronium ( $\text{H}_3\text{O}^+$ ) as the primary reagent ion (Lindinger et al., 1993). In this instance, the hydronium ions were generated from a humidified  $\text{N}_2$  (N6.0) carrier gas. Providing certain reaction conditions are met, ion molecule reaction between  $\text{H}_3\text{O}^+$  and the organic analyte will yield a

## Investigating the use of secondary organic aerosol

J. F. Hamilton et al.

Title Page

Abstract

Introduction

Conclusions

References

Tables

Figures

◀

▶

◀

▶

Back

Close

Full Screen / Esc

Printer-friendly Version

Interactive Discussion





protonated product ion ( $\text{RH}^+$ ) and neutral water;



Despite being considered a relatively *soft* ionisation method, the nascent  $\text{RH}^+$  ion may be sufficiently energetic so as to dissociate and produce one or more fragment ions (Blake et al., 2009).

Chamber air containing the analyte was delivered in a continuous stream (approximately 230 sccm) to the drift cell *via* a 0.5 m long, 1/4 (internal diameter) Teflon sample line, heated to 40 ( $\pm 1$ ) °C. The centre drift cell was operated at an  $E/N$  (i.e. electric field/gas number density) ratio of approximately 90 Td. An energy ramp was applied at the base of the cell to remove potential water-cluster ions (e.g.  $\text{RH}^+ \cdot \text{H}_2\text{O}$ ). The CIR-TOF-MS was calibrated *via* three separate methods: (i) using step-wise dilution of a gravimetrically prepared gas standard (BOC Special Gases, UK) containing a variety of VOCs and oxygenated (O)VOCs; (ii) using calibration material produced in-house *via* the injection of liquid samples (prepared by volumetric dilution of the pure material in hexane) into 10 l Tedlar bags (SKC Inc., USA) containing both humidified and dry, pure nitrogen; and (iii) using gaseous standards derived from permeation tubes (Vici Inc., US; Eco-scientific, UK), diluted, humidified and delivered to the CIR-TOF-MS by a commercial calibration unit (Kintec, model: 491).

## 2.4 Aerosol characterisation

The total SOA particle number concentration was measured using an ultrafine water-based condensation particle counter (wCPC 3786, TSI, Inc.). This model has a minimum size cut-off of 2.5 nm. The size distribution of the generated SOA particles was measured using a Differential Mobility Particle Sizer (DMPS). The DMPS instrument consists of two Vienna design Differential Mobility Analysers (DMAs) (Williams, 1999): an ultrafine DMA for particles in the size range 3.4–34 nm and a standard DMA for particle sizes from 20–500 nm. After transmission through the DMAs, particles are counted

## Investigating the use of secondary organic aerosol

J. F. Hamilton et al.

Title Page

Abstract

Introduction

Conclusions

References

Tables

Figures

◀

▶

◀

▶

Back

Close

Full Screen / Esc

Printer-friendly Version

Interactive Discussion



using condensation particle counters (CPC). The ultrafine DMA was attached to a TSI 3025A CPC and the standard DMA to a TSI 3010 CPC. The DMAs were operated in parallel and utilised a custom built sealed, recirculating sheath air system, which was dried and filtered. Particle size distributions in the diameter size range from 3 nm to 500 nm were obtained every 10 min.

A hygroscopicity tandem differential mobility analyser (HTDMA) was used to measure on-line size resolved water uptake at 90% RH. The HTDMA dries the sample aerosol to <10% RH using a Nafion® drier (Perma Pure, MD-110-12, Toms River, NJ, USA). A Strontium-90 aerosol neutraliser then brings the sample into charge equilibrium. A DMA (BMI, Haywood, CA, USA) operated with a re-circulating sheath flow of 5 L min<sup>-1</sup> and sample flow of 0.5 L min<sup>-1</sup> selects particles of a single mobility. Diameters chosen were larger than the mode of the number size distribution, thus avoiding the sampling of a significant fraction of multi-charged particles. The sample is then humidified to 90% RH using a Gore-Tex® humidifier (Cubison et al., 2006). The humidified size selected sample is then passed through a residence coil for 15 s. A second DMA (BMI) and CPC (TSI, 3782) is then used to measure the size distribution of the humidified sample using the DMPS technique. The temperature of the DMAs and humidification system is controlled using peltier units (Supercool®, AA-040-12-22, Sweden). The humidity is measured using a dew point hygrometer (EdgeTech, Dewmaster, MA, USA). The operation of the HTDMA was validated by sampling ammonium sulphate and sodium chloride test aerosols using the operating procedures described by Good et al. (2010). The data was inverted using the method described by Gysel et al. (2009). The data from the HTDMA is reported in terms of the hygroscopic growth factor ( $GF_{D_0, RH}$ ), the wet particle diameter at a given RH divided by the particle's dry diameter ( $D_0$ ). The aerosol particles measured appeared internally mixed, hence the reported growth factors are the number weighted means of the measured growth factor probability density distributions unless otherwise stated (Gysel et al., 2009).

Measurements of the secondary organic aerosol composition were made using a compact Time-of-flight Aerosol Mass Spectrometer (Drewnick et al., 2005) (cToF-AMS,

## Investigating the use of secondary organic aerosol

J. F. Hamilton et al.

Title Page

Abstract

Introduction

Conclusions

References

Tables

Figures

◀

▶

◀

▶

Back

Close

Full Screen / Esc

Printer-friendly Version

Interactive Discussion



Aerodyne Research Inc., USA). The instrument operated in the standard configuration, taking both mass spectrum (MS) and particle time-of-flight (pToF) data, and was calibrated using 350 nm monodisperse ammonium nitrate particles. A more detailed description of the instrument and its calibration was provided by Drewnick et al. (2005).

The detailed chemical composition of the SOA was determined from filter samples using two complementary techniques. The semi-volatile fraction of the SOA was analysed using direct thermal desorption coupled to GC×GC-TOF/MS. A small piece of the filter (10–20 mg) was cut out, placed inside a thermal desorption glass vial and injected using an autosampler. Two stage thermal desorption was used to ensure a narrow band of analytes was injected onto the column (MPS2 autosampler and TDU/CIS4, Gerstel, Germany). GC × GC-TOF/MS was carried out using a cryo-jet Pegasus 4D (Leco, St. Joseph, MI, USA) incorporating an Agilent 6890N Gas Chromatograph and a Pegasus III reflectron time-of-flight mass spectrometer. A liquid nitrogen cooled gas jet midpoint modulator, at approximately  $-160^{\circ}\text{C}$ , was used to enable comprehensive two-dimensional separations. A secondary oven housed within the GC oven allowed independent column temperature control. The column set used in these experiments provides a primary volatility based separation followed by a secondary polarity based separation. The first dimension was a 5% phenyl- 95% methyl-polysiloxane 30 m × 320  $\mu\text{m}$  × 1.0  $\mu\text{m}$  HP-5 (J&W Scientific, Wilmington, DE, USA). The second column was a 50% phenyl-polysiloxane 2 m × 100  $\mu\text{m}$  × 0.1  $\mu\text{m}$  BP10 (SGE, Melbourne, Australia). The GC was held at  $70^{\circ}\text{C}$  for two minutes and then raised at  $2.5^{\circ}\text{C min}^{-1}$  to  $250^{\circ}\text{C}$  and held at this temperature for a further sixteen minutes. The carrier gas was helium (99.9999%, BOC Gases, Guildford, UK) supplied at  $1.5\text{ ml min}^{-1}$ . The modulator and secondary oven were operated at  $+30^{\circ}\text{C}$  and  $+15^{\circ}\text{C}$  above GC oven temperature, respectively.

The remainder of the filter sample was extracted into high purity water, filtered and reduced to 1 ml using a vacuum solvent evaporator (Biotage, Sweden). The water soluble and high molecular weight compounds were analysed using liquid chromatography-ion trap mass spectrometry (LC-MS<sup>n</sup>). LC-MS was carried out using an HCT Plus ion

## Investigating the use of secondary organic aerosol

J. F. Hamilton et al.

Title Page

Abstract

Introduction

Conclusions

References

Tables

Figures

◀

▶

◀

▶

Back

Close

Full Screen / Esc

Printer-friendly Version

Interactive Discussion



trap mass spectrometer (Bruker Daltonics GmbH, Bremen, Germany) equipped with an Eclipse ODS-C<sub>18</sub> column with 5 μm particle size (Agilent, 4.6 mm×150 mm). Both positive and negative ionisation modes were used. Full details of the methodology and instrument have been published previously (Hamilton et al., 2008).

5 Samples were also analysed at high resolution using a Bruker APEX 9.4 T Fourier Transform Ion Cyclotron Resonance Mass Spectrometer. Extracts were sprayed at a flow rate of 2 μL min<sup>-1</sup>, into an Apollo II electrospray interface with ion funnelling technology. Spectra were acquired in both positive and negative ion mode over the scan range *m/z* 100–3000 using the following MS parameters: nebulising gas flow: 0.9 L min<sup>-1</sup>, drying gas flow: 5 L min<sup>-1</sup>, drying temperature: 190 °C, collision cell accumulation: 0.05–0.5 s, and data acquisition size: 2 MW (yielding a target resolution of 130 000 at *m/z* 400). Data were analysed using DataAnalysis 4.0 software (Bruker Daltonics, Bremen, Germany). The instrument was calibrated using protonated (positive ion mode) or deprotonated (negative ion mode) arginine clusters. The mass spectra were internally recalibrated with a series of prominent peaks: positive – C<sub>10</sub>H<sub>16</sub>NaO<sub>3</sub>, C<sub>12</sub>H<sub>20</sub>NaO<sub>3</sub>, C<sub>13</sub>H<sub>22</sub>NaO<sub>3</sub>, C<sub>14</sub>H<sub>22</sub>NaO<sub>3</sub>, C<sub>14</sub>H<sub>22</sub>NaO<sub>4</sub>, C<sub>16</sub>H<sub>28</sub>NaO<sub>4</sub>; negative – C<sub>10</sub>H<sub>15</sub>O<sub>5</sub>, C<sub>9</sub>H<sub>14</sub>O<sub>4</sub>, C<sub>10</sub>H<sub>15</sub>O<sub>4</sub>, C<sub>10</sub>H<sub>16</sub>O<sub>5</sub>, C<sub>14</sub>H<sub>22</sub>O<sub>4</sub>. Background contaminants also seen in pure water and blank extracted filters were removed and intensity weighted O:C and H:C ratios were calculated. Three dimensional Van Krevelen plots were created in IDL v6.3 (ITTVIS), with data displayed in contour plots over 10 contour levels. Data were interpolated between sample points and the intensity scaled to 70% of the maximum value.

### 3 Results and discussion

25 The experimental details are given in Table 1. A typical experiment is split into three phases:

## Investigating the use of secondary organic aerosol

J. F. Hamilton et al.

Title Page

Abstract

Introduction

Conclusions

References

Tables

Figures

◀

▶

◀

▶

Back

Close

Full Screen / Esc

Printer-friendly Version

Interactive Discussion



- In phase 1, the  $\beta$ -caryophyllene was introduced, the lights turned on and SOA formed.
- In phase 2, the lights were turned off, the chamber was flushed to reduce seed and VOC concentrations, then diluted with clean air while the limonene was injected into the chamber.
- In phase 3, the lights were turned on and limonene photo-oxidation occurred followed by product condensation onto the organic seed.

The evolution of certain key parameters is shown in Fig. 1 for a typical example of the organic seed experiments (25 June 2008). In Fig. 1, the beginning of Phase 1 occurs at time = 0 and the vertical red dotted lines show the beginning and end of phase 2. In this experiment 34 ( $\pm 1$ ) ppbV  $\text{NO}_x$  (in the form of NO and  $\text{NO}_2$ ) and 49 ( $\pm 9$ ) ppbV of  $\beta$ -caryophyllene were introduced into the chamber to give an initial VOC/ $\text{NO}_x$  ratio of approximately 1.4. Following injection of the reactants the chamber lights were turned on (at time = 0) and almost immediately the SOA mass in the chamber was observed to increase. The SOA number density peaked after 10 min and the mass peaked at around  $36 \mu\text{g m}^{-3}$  after 60 min. A density of 1.3 was used for both the  $\beta$ -caryophyllene and limonene SOA based on the most recent literature to calculate the SOA mass from the DMPS volume data (Bahreini et al., 2005; Varutbangkul et al., 2006). Very little ozone was observed to accumulate within the chamber during Phase 1, (maximum of 8 ( $\pm 2$ ) ppbV at the end of Phase 1) owing to its rapid reaction with the  $\beta$ -caryophyllene (lifetime of  $\beta$ -caryophyllene with  $\text{O}_3$  is around 2 min). In comparison with other VOC chamber photo-oxidation systems (Odum et al., 1997),  $\beta$ -caryophyllene chamber photo-oxidation results in relatively unusual  $\text{NO}_x$  chemistry, which will be discussed in more detail in a future publication (Alfarra et al., 2010). In brief however, the  $\text{NO}_x$  behaviour observed in Fig. 1 may be a result of the fast reaction rate of  $\beta$ -caryophyllene with ozone and resultant low radical yields.

Following near complete reaction of the  $\beta$ -caryophyllene (98–99% oxidation), the chamber was then diluted to leave a  $\beta$ -caryophyllene organic seed aerosol background

## Investigating the use of secondary organic aerosol

J. F. Hamilton et al.

[Title Page](#)[Abstract](#)[Introduction](#)[Conclusions](#)[References](#)[Tables](#)[Figures](#)[◀](#)[▶](#)[◀](#)[▶](#)[Back](#)[Close](#)[Full Screen / Esc](#)[Printer-friendly Version](#)[Interactive Discussion](#)

of approximately  $4 \mu\text{g m}^{-3}$ . No change in particle size (due to revolatilisation) was seen during dilution, indicating that the  $\beta$ -caryophyllene SOA was mostly composed of low volatility compounds. Figure 2 shows a comparison of SOA size distributions measured immediately before the lights were turned off at the end of Phase 1 (before dilution) and the immediately before lights were turned back on at the start of Phase 3 (after dilution). Grieshop et al., 2007 showed that SOA from  $\alpha$ -pinene ozonolysis repartitions reversibly upon dilution, but on a much longer time scale than has been observed in single component aerosols of similar sizes. Our dilution time scale was much shorter and did not lead to any volatilisation of SOA. During Phase 2, ozone levels in the chamber dropped below the detection limit of the instrument (2 ppbV), indicating that the ozone mixing ratio was near zero before the start of phase 3. Following dilution, 93 ( $\pm 10$ ) ppbV of limonene was injected into the chamber before an additional “top-up” injection of  $\text{NO}_x$  was added (in the form of  $\text{NO}_2$ ) to ensure an initial  $\text{VOC}/\text{NO}_x$  ratio similar to that of Phase 1 (i.e.  $\sim 2.0$ ). On average for the three experiments, less than 0.5 ( $\pm 1$ ) ppbV of  $\beta$ -caryophyllene remained in the chamber following dilution. Also, from the application of a pseudo calibration sensitivity to the data (obtained for the  $\text{C}_{10}$  multifunctional monoterpene oxidation product, pinonaldehyde), it is estimated that an average of only 2–3 ( $\pm 1$ ) ppbV of  $\beta$ -caryophyllene oxidation products were carried over to Phase 3 of the experiment. In addition, complete evaporation of the seed particle post-dilution could only have contributed to a maximum of 0.5 ppbV of the caryophyllenic VOC observed; in practice this would be very much lower.

Limonene oxidation was observed by the CIR-TOF-MS during Phase 3 of the experiment, after chamber lights had been switched back on. For all experiments limonene was quantified from the spectral signal corresponding to the protonated limonene parent ion ( $m/z$  137). During Phase 3, the decay of limonene was matched by the concomitant production of its gas phase reaction products, including limonaldehyde ( $m/z$  169, 151 and 107) and limonaketone ( $m/z$  139). The oxidation of limonene and the production of limonaldehyde are shown in Fig. 1. Limonene oxidation and limonaldehyde formation was reproducible between experiments, with approximately all of the

## Investigating the use of secondary organic aerosol

J. F. Hamilton et al.

[Title Page](#)[Abstract](#)[Introduction](#)[Conclusions](#)[References](#)[Tables](#)[Figures](#)[⏪](#)[⏩](#)[◀](#)[▶](#)[Back](#)[Close](#)[Full Screen / Esc](#)[Printer-friendly Version](#)[Interactive Discussion](#)

limonene reacted by the end of phase 3 (i.e. after 240 min) in each instance and limon-  
aldehyde formed in molar yields of  $\sim 7$ –14%. The formation of ozone and more con-  
ventional chamber  $\text{NO}_x$  chemistry observed during Phase 3 can also be seen in Fig. 1,  
with a maximum of 35 ( $\pm 2$ ) ppb of ozone produced. The SOA mass (as well as seed  
particle size) increased steadily from lights on until 240 min, where a second nucleation  
event was seen, with a steep jump in the particle number concentrations. This can be  
seen in the particle size distribution shown in Fig. 3.

It is clear from Fig. 1 that limonene oxidation products are partitioning onto the or-  
ganic seed aerosol increasing aerosol mass from  $4 \mu\text{g m}^{-3}$  to  $70 \mu\text{g m}^{-3}$ , giving an  
average mass growth of  $34.5 \mu\text{g m}^{-3} \text{ h}^{-1}$ . The particles grew from 150 to 325 nm mean  
diameter during the first 50 min after lights on in Phase 3, as shown in Fig. 3, giving  
an average size growth of  $3.5 \text{ nm min}^{-1}$ . The formation of small particles in the second  
nucleation event effectively reduces further uptake onto the seed particles. In order  
to suppress the limonene nucleation, a series of experiments were carried out under  
different conditions, including reducing the amount of limonene to 21 ( $\pm 4$ ) ppb in one  
experiment and increasing the amount of organic seed to  $13 \mu\text{g m}^{-3}$  in another. In all  
cases, limonene nucleation could not be suppressed. Potential reasons for this may  
include the following; (i) there is insufficient particle mass onto which the limonene ox-  
idation products can absorb, (ii) the loss of such limonene oxidation products to seed  
surface area is slower than the production of condensable material, meaning the par-  
tial pressure increases sufficiently high to exceed the nucleation threshold, (iii) the  $n$ -th  
generation oxidation product is so condensable that its partial pressure increase to re-  
latively low values, which are above the nucleation threshold and (iv) one or more of the  
limonene OVOCs are not fully miscible in the  $\beta$ -caryophyllene SOA products such that  
they would prefer to be in the gas phase until they build up to concentrations above  
the nucleation threshold. To allow comparison of limonene SOA composition formed  
from nucleation only and from an organic seeded experiment, the experiment could  
be stopped immediately as new particle formation was observed and a filter was col-  
lected. This would minimise the mass of limonene nucleation SOA collected in seeded

## Investigating the use of secondary organic aerosol

J. F. Hamilton et al.

[Title Page](#)[Abstract](#)[Introduction](#)[Conclusions](#)[References](#)[Tables](#)[Figures](#)[◀](#)[▶](#)[◀](#)[▶](#)[Back](#)[Close](#)[Full Screen / Esc](#)[Printer-friendly Version](#)[Interactive Discussion](#)



experiments and will be carried out in future studies.

$\beta$ -Caryophyllene photo-oxidation during Phase 1 of the organic seed experiments resulted in the production of a peak SOA mass of the order 36–66  $\mu\text{g m}^{-3}$ , between 40 and 60 min after initial lights on (see Table 1). Substituting these masses into (R2), along with the fraction of  $\beta$ -caryophyllene reacted, allows the SOA yield ( $Y_{\text{SOA}}$ ) to be determined:

$$Y_{\text{SOA}} = \frac{M_P}{\Delta\text{VOC}} \quad (\text{R2})$$

For Phase 1 of the seed experiments,  $Y_{\text{SOA}}$  was determined to be of the order 10–19%. During Phase 3 of the experiments, the condensation of limonene photo-oxidation products onto the  $\beta$ -caryophyllene seed resulted in the production of an additional 7–65  $\mu\text{g m}^{-3}$  of SOA mass on top of the seed, such that the peak mass was measured to be 13–70  $\mu\text{g m}^{-3}$  between 110 and 135 min after second lights on, giving  $Y_{\text{SOA}}$  for the condensed mass of the order 6–14%. Owing to the lack of appropriate data, these mass and yield values have not been wall loss corrected. Recent work (Matsunaga and Ziemann, 2010) has shown that wall losses of SVOC may be significant in chamber studies and so the yields presented here are expected to a lower limit for these experiments, particularly in the case of the higher molecular weight  $\beta$ -caryophyllene.

The hygroscopic growth at 90% RH was measured by the HTDMA. In order to measure the effect of partitioning to the seed, a series of nucleation only experiments were carried out for both  $\beta$ -caryophyllene and limonene. These single precursor experiments were for nominal mixing ratios of 50 ppb and 250 ppb and selected dry particle diameters between 50 nm and 500 nm. The growth factor of the pure  $\beta$ -caryophyllene SOA ranged from 1.00 to 1.06 in the 5-th to 95-th percentile range when binned at 60 min intervals from 30 min after lights on (illustrated in Fig. 4 upper panel) over 8 separate experiments. Ageing resulted in a small increase in the growth factor over 270 min. The growth factor of the pure limonene SOA ranged from 1.11 to 1.27 (also binned at 60 min intervals) in the 5-th to 95-th percentile range (illustrated in Fig. 4

Investigating the use of secondary organic aerosol

J. F. Hamilton et al.

Title Page

Abstract

Introduction

Conclusions

References

Tables

Figures

◀

▶

◀

▶

Back

Close

Full Screen / Esc

Printer-friendly Version

Interactive Discussion





**Investigating the use  
of secondary organic  
aerosol**

J. F. Hamilton et al.

Title Page

Abstract

Introduction

Conclusions

References

Tables

Figures

◀

▶

◀

▶

Back

Close

Full Screen / Esc

Printer-friendly Version

Interactive Discussion



upper panel) over 6 experiments, with an increase mainly within the first 120 min due to ageing. The lower panel in Fig. 4 shows the growth factor measured during the 25 June 2008 limonene on  $\beta$ -caryophyllene seed experiment. When the  $\beta$ -caryophyllene aerosol was diluted for use as a seed its hygroscopic growth didn't change significantly from its undiluted behaviour. After the limonene injection and lights on, condensation of limonene oxidation products on to the seed results in a rapid increase in the growth factor. Several hours after the limonene injection the growth factors were comparable to those measured in the limonene nucleation experiments.

The bulk composition of the  $\beta$ -caryophyllene seed was investigated using a c-ToF-AMS. The relative abundance of the ion signal  $m/z$  44 expressed as a fraction of total organic signal ( $f_{44}$ ) has been widely used as a proxy for the level of oxygenation of organic aerosols (Alfarra et al., 2004, 2006, 2007). Mass fragment 44 is due mostly to the ion fragment  $\text{CO}_2^+$ , and has previously been shown to strongly correlate with organic O:C for ambient and chamber OA (Aiken et al., 2008). For the  $\beta$ -caryophyllene seed,  $f_{44}$  was found to be 4.6% at the end of Phase 1, indicating a low degree of oxidation, as expected if first generation products are nucleating to form the seed within 5 min of lights on (see Fig. 3). Compositional analysis indicated that the main  $\beta$ -caryophyllene oxidation species in the seed were  $\beta$ -caryophyllonic acid and  $\beta$ -caryophyllinic acid, which are first generation products, in contrast to the recent work of Li et al. (2010). When limonene oxidation products condense onto the seed in Phase 3,  $f_{44}$  increases rapidly to 7.4%, showing that limonene SOA is much more oxidised than the seed. It can be seen in Fig. 3 that the seed ages slowly with a steady increase in  $f_{44}$  during Phase 1 to a final value of 4.6% after 3 h. The addition of limonene SOA resulted in a much steeper jump in the degree of oxidation of the aerosol, confirming this increase is not due to seed processing.

The detailed composition of the seed and the limonene SOA + seed were investigated using two offline techniques, GC  $\times$  GC-TOF/MS and LC-MS<sup>n</sup>. GC  $\times$  GC has been successfully used to study chamber generated SOA for a range of precursors (Hamilton et al., 2005, 2010). The GC  $\times$  GC chromatograms obtained by thermal desorption of

5 both seed and limonene filter samples are shown in Fig. 5, where the  $x$ - and  $y$ -axis represents retention time on column 1 and 2, respectively and response is indicated by a coloured contour. The chromatograms shown are extracted ion plots of  $m/z$  93 + 91, which are strong terpene fragments. In the GC  $\times$  GC set up used, increasing retention time on column 1 indicates decreasing volatility and increasing retention time on column 2 indicates increasing polarity. The  $\beta$ -caryophyllene seed chromatogram in Fig. 5a, has a complex composition, with the highest concentration of spots circled in yellow. The position of the seed spots on the contour plot indicates that this is low volatility and low polarity material. MS fragmentation patterns can be used to identify a small number of components, but there are very few appropriate EI spectra available for comparison. As shown in Fig. 5, there is a clear difference between the chromatogram of the  $\beta$ -caryophyllene seed and the limonene SOA + seed sample, with an increased number of species present in the latter. The majority of the limonene SOA, shown within the pink circle of Fig. 5b, has a lower retention time on column 1 and an increased retention time on column 2, indicating that it is more volatile and more polar than the seed, respectively. This correlates well with the increase in  $f_{44}$  seen in the AMS spectra.  $\beta$ -caryophyllene is therefore a useful material to use as the seed for studying monoterpene SOA owing to its higher molecular weight, which allows a clear distinction from the condensing organics. The high polar resolving power of GC  $\times$  GC has a clear advantage for these samples over conventional GC-MS. However, the desorption temperature of the GC technique (350 °C) is insufficient to volatilise the least volatile  $\beta$ -caryophyllene SOA components and thus a complementary technique is required.

25 LC-MS has also been used to investigate the composition of the water soluble extracts of the two samples. Positive ionisation, where all peaks exist as their  $[M+Na]^+$  adducts, was used to provide a response for the widest range of functionalities. All mass spectra across the entire LC retention time were averaged (reducing artefact formation from direct ESI analysis) to obtain a molecular weight distribution representing the seed and the limonene SOA + seed and these are shown in Fig. 6. The  $m/z$  axis

**Investigating the use of secondary organic aerosol**

J. F. Hamilton et al.

Title Page

Abstract

Introduction

Conclusions

References

Tables

Figures

◀

▶

◀

▶

Back

Close

Full Screen / Esc

Printer-friendly Version

Interactive Discussion



has been shifted by 23 Da to give the molecular weight rather than the adduct ion mass. The  $\beta$ -caryophyllene seed mass spectrum, shown in Fig. 6 (upper panel), is dominated by compounds in the range 238 to 300 Da. Using LC-MS<sup>n</sup> to separate and fragment these species indicates they are primarily first and second generation products of OH and O<sub>3</sub> chemistry. The major peaks are 238, 254, 270 and 284 and peak assignment and molecular identification will be provided in a companion manuscript (Alfarra et al., 2010). The limonene SOA + seed mass spectrum, shown in Fig. 6 (middle panel), shows the appearance of lower molecular weight limonene oxidation products in the range 140 to 234 Da. A reduction in the intensity of the seed ions (i.e. 254, 270 etc.) was observed and this is to be expected considering that the seed has been diluted in the chamber and would have been further diluted by the limonene SOA. In order to pull out the mass channels corresponding to the limonene SOA, a difference spectrum was created as shown in Fig. 6c, where peaks more abundant in the seed have negative values on the y-axis and peaks more abundant in the limonene + seed SOA have positive values on the y-axis. The total ion intensity was normalised to the amount of aerosol collected to allow a comparison of relative composition. The major limonene peaks detected correspond to molecular weights of 170, 186, 200 and 216 Da. The limonene SOA mass channels were subsequently investigated further using LC-MS<sup>n</sup> to allow identification of limonene oxidation products in the aerosol. Using fragmentation patterns a total of 14 limonene products were identified and these are shown in Table 2.

FTICR-MS was used in negative mode to determine molecular formulae for each peak with a relative intensity greater than 0.3% of the base peak. Peaks were assumed to contain only C, H and O and molecular formulae were converted into H:C and O:C ratios. Comparison of the results with a chamber background indicated that a number of peaks were due to contamination. These were identified as saturated fatty acids from the solvents used (not seen in GC  $\times$  GC) and these ions were removed from any further analysis. A further manual inspection of molecular formulae was used to remove unrealistic assignments, based on maximum O:C = 2 and the degree of unsaturation

## Investigating the use of secondary organic aerosol

J. F. Hamilton et al.

[Title Page](#)[Abstract](#)[Introduction](#)[Conclusions](#)[References](#)[Tables](#)[Figures](#)[◀](#)[▶](#)[◀](#)[▶](#)[Back](#)[Close](#)[Full Screen / Esc](#)[Printer-friendly Version](#)[Interactive Discussion](#)

(rings + double bonds). Rather than investigate the detailed composition, a bulk view of the degree of oxidation was used for comparison by plotting 3-D Van Krevelen diagrams, where the  $x$ - and  $y$ -axis represent the O:C and H:C ratios respectively and a coloured contour is used to represent peak intensity. Although peak intensity does not scale exactly with concentration, a comparison of the relative intensity patterns is still informative. The 3-D Van Krevelen diagrams for the seed and limonene SOA + seed are shown in Fig. 7. The seed plot shows a narrow O:C range between approximately 0.1 and 0.4 with an intensity weighted mean value of 0.32. The peaks take up a very narrow region of the Van Krevelen space. In contrast, the limonene SOA + seed is more spread out, with some molecules having much higher O:C ratios. The O:C range was between 0.1 and 0.8 and the intensity weight mean was 0.37. It is also apparent that the degree of unsaturation increases with an increase in lower H:C values. A similar increase of 0.05 is also seen in positive ionisation mode. Limonene oxidation products are therefore smaller and more polar, which will in turn increase their water solubility. This may lead to a further skewing of the O:C ratio. However, it is clear that the  $\beta$ -caryophyllene first generation products are still sufficiently water soluble to be extracted. An increase in O:C and decrease in H:C should result in an increase in hygroscopicity which is indeed seen to be the case here. The data falls nicely within the O:C *versus* GF relationship shown in Jimenez et al., 2009, however this may not be the case for other precursors.

There is some evidence for the formation of limonene +  $\beta$ -caryophyllene oligomers. For example, a peak at  $m/z$  455.2654 is identified as  $C_{24}H_{39}O_8$ , which could be a combination of a  $C_{10}$  (limonene) and a  $C_{14}$  ( $\beta$ -caryophyllene) oxidation product. However, high molecular weight species ( $m/z > 350$  Da) represent less than 5% of the total peak intensity. These species are not seen in the LC-MS mass spectra and it is impossible at this time to rule out the formation of adducts during electrospray ionisation.

## Investigating the use of secondary organic aerosol

J. F. Hamilton et al.

Title Page

Abstract

Introduction

Conclusions

References

Tables

Figures

◀

▶

◀

▶

Back

Close

Full Screen / Esc

Printer-friendly Version

Interactive Discussion



## 4 Conclusions

In order to improve current simulation of SOA formation, atmospherically representative seed particles are required. This work has shown that  $\beta$ -caryophyllene SOA generated in situ in the chamber shows promise as a more realistic organic seed particle. It can be formed quickly, is relatively stable, cheap and easy to use. The relatively high molecular weight of the seed constituents leads to components that can be separated from the oxidation products of common VOC such as isoprene, monoterpenes and aromatics without the need for expensive isotopic labelling. Limonene SOA formation was studied using this seed and a clear change in the aerosol properties was observed during photo-oxidation and subsequent gas-particle partitioning. The  $f_{44}$  from the AMS and the O:C ratio obtained from the FTICR-MS both indicate that limonene SOA is more polar and more oxidised than the seed and this resulted in an increase in hygroscopicity of the particles. This type of experiment could be used in the future to study the effect of the seed on limonene SOA composition by comparison to nucleation type experiments.

*Acknowledgements.* The authors gratefully acknowledge the UK Natural Environment Research Council for funding of the ACES project (NE/E011160/1) and the APPRAISE program. FTICR-MS measurements were made by Ed Bergström, University of York using facilities available in the Centre of Excellence in Mass Spectrometry. The York Centre of Excellence in Mass Spectrometry was created thanks to a major capital investment through Science City York, supported by Yorkshire Forward with funds from the Northern Way Initiative.

## References

Aiken, A. C., DeCarlo, P. F., Kroll, J. H., Worsnop, D. R., Huffman, J. A., Docherty, K. S., Ulbrich, I. M., Mohr, C., Kimmel, J. R., Sueper, D., Sun, Y., Zhang, Q., Trimborn, A., Northway, M., Ziemann, P. J., Canagaratna, M. R., Onasch, T. B., Alfarra, M. R., Prevot, A. S. H., Dommen, J., Duplissy, J., Metzger, A., Baltensperger, U., and Jimenez, J. L.: O/C and OM/OC ratios of primary, secondary, and ambient organic aerosols with high-resolution time-of-flight aerosol mass spectrometry, *Environ. Sci. Technol.*, 42, 4478–4485, 2008.

### Investigating the use of secondary organic aerosol

J. F. Hamilton et al.

Title Page

Abstract

Introduction

Conclusions

References

Tables

Figures



Back

Close

Full Screen / Esc

Printer-friendly Version

Interactive Discussion



**Investigating the use  
of secondary organic  
aerosol**

J. F. Hamilton et al.

Title Page

Abstract

Introduction

Conclusions

References

Tables

Figures

◀

▶

◀

▶

Back

Close

Full Screen / Esc

Printer-friendly Version

Interactive Discussion



- Alfarra et al.: The effect of ageing on the composition and hygroscopic properties of secondary organic aerosol formed during beta-caryophyllene photooxidation, 2010.
- Alfarra, M. R., Coe, H., Allan, J. D., Bower, K. N., Boudries, H., Canagaratna, M. R., Jimenez, J. L., Jayne, J. T., Garforth, A. A., Li, S. M., and Worsnop, D. R.: Characterization of urban and rural organic particulate in the lower Fraser valley using two aerodyne aerosol mass spectrometers, *Atmos. Environ.*, 38, 5745–5758, 2004.
- Alfarra, M. R., Paulsen, D., Gysel, M., Garforth, A. A., Dommen, J., Prévôt, A. S. H., Worsnop, D. R., Baltensperger, U., and Coe, H.: A mass spectrometric study of secondary organic aerosols formed from the photooxidation of anthropogenic and biogenic precursors in a reaction chamber, *Atmos. Chem. Phys.*, 6, 5279–5293, doi:10.5194/acp-6-5279-2006, 2006.
- Bahreini, R., Keywood, M. D., Ng, N. L., Varutbangkul, V., Gao, S., Flagan, R. C., Seinfeld, J. H., Worsnop, D. R., and Jimenez, J. L.: Measurements of secondary organic aerosol from oxidation of cycloalkenes, terpenes, and m-xylene using an Aerodyne aerosol mass spectrometer, *Environ. Sci. Technol.*, 39, 5674–5688, 2005.
- Blake, R. S., Monks, P. S., and Ellis, A. M.: Proton-Transfer Reaction Mass Spectrometry, *Chem. Rev.*, 109, 861–896, 2009.
- Blake, R. S., Whyte, C., Hughes, C. O., Ellis, A. M., and Monks, P. S.: Demonstration of proton-transfer reaction time-of-flight mass spectrometry for real-time analysis of trace volatile organic compounds, *Anal. Chem.*, 76, 3841–3845, 2004.
- Capes, G., Murphy, J. G., Reeves, C. E., McQuaid, J. B., Hamilton, J. F., Hopkins, J. R., Crosier, J., Williams, P. I., and Coe, H.: Secondary organic aerosol from biogenic VOCs over West Africa during AMMA, *Atmos. Chem. Phys.*, 9, 3841–3850, doi:10.5194/acp-9-3841-2009, 2009.
- Corrigan, A. L., Hanley, S. W., and Haan, D. O.: Uptake of glyoxal by organic and inorganic aerosol, *Environ. Sci. Technol.*, 42, 4428–4433, 2008.
- Cubison, M. J., Alfarra, M. R., Allan, J., Bower, K. N., Coe, H., McFiggans, G. B., Whitehead, J. D., Williams, P. I., Zhang, Q., Jimenez, J. L., Hopkins, J., and Lee, J.: The characterisation of pollution aerosol in a changing photochemical environment, *Atmos. Chem. Phys.*, 6, 5573–5588, doi:10.5194/acp-6-5573-2006, 2006.
- Dommen, J., Hellelūn, H., Saurer, M., Jaeggi, M., Siegwolf, R., Metzger, A., Duplissy, J., Fierz, M., and Baltensperger, U.: Determination of the Aerosol Yield of Isoprene in the Presence of an Organic Seed with Carbon Isotope Analysis, *Environ. Sci. Technol.*, 43, 6697–6702, 2009.

**Investigating the use of secondary organic aerosol**

J. F. Hamilton et al.

Title Page

Abstract

Introduction

Conclusions

References

Tables

Figures

◀

▶

◀

▶

Back

Close

Full Screen / Esc

Printer-friendly Version

Interactive Discussion



- Drewnick, F., Hings, S. S., DeCarlo, P., Jayne, J. T., Gonin, M., Fuhrer, K., Weimer, S., Jimenez, J. L., Demerjian, K. L., Borrmann, S., and Worsnop, D. R.: A new time-of-flight aerosol mass spectrometer (TOF-AMS) – Instrument description and first field deployment, *Aerosol Sci. Technol.*, 39, 637–658, 2005.
- 5 Fuzzi, S., Andreae, M. O., Huebert, B. J., Kulmala, M., Bond, T. C., Boy, M., Doherty, S. J., Guenther, A., Kanakidou, M., Kawamura, K., Kerminen, V.-M., Lohmann, U., Russell, L. M., and Pöschl, U.: Critical assessment of the current state of scientific knowledge, terminology, and research needs concerning the role of organic aerosols in the atmosphere, climate, and global change, *Atmos. Chem. Phys.*, 6, 2017–2038, doi:10.5194/acp-6-2017-2006, 2006.
- 10 Good, N., Coe, H., and McFiggans, G.: Instrumentational operation and analytical methodology for the reconciliation of aerosol water uptake under sub- and supersaturated conditions, *Atmos. Meas. Tech.*, 3, 1241–1254, doi:10.5194/amt-3-1241-2010, 2010.
- Grieshop, A. P., Donahue, N. M., and Robinson, A. L.: Is the gas-particle partitioning in alpha-pinene secondary organic aerosol reversible?, *Geophys. Res. Lett.*, 34, L14810, doi:10.1029/2007GL029987, 2007.
- 15 Gysel, M., McFiggans, G. B., and Coe, H.: Inversion of tandem differential mobility analyser (TDMA) measurements, *J. Aerosol Sci.*, 40, 134–151, 2009.
- Hallquist, M., Wenger, J. C., Baltensperger, U., Rudich, Y., Simpson, D., Claeys, M., Dommen, J., Donahue, N. M., George, C., Goldstein, A. H., Hamilton, J. F., Herrmann, H., Hoffmann, T., Iinuma, Y., Jang, M., Jenkin, M. E., Jimenez, J. L., Kiendler-Scharr, A., Maenhaut, W., McFiggans, G., Mentel, Th. F., Monod, A., Prévôt, A. S. H., Seinfeld, J. H., Surratt, J. D., Szmigielski, R., and Wildt, J.: The formation, properties and impact of secondary organic aerosol: current and emerging issues, *Atmos. Chem. Phys.*, 9, 5155–5236, doi:10.5194/acp-9-5155-2009, 2009.
- 20 Hamilton, J. F.: Using Comprehensive Two-Dimensional Gas Chromatography to Study the Atmosphere, *J. Chromat. Sci.*, 48, 274–282, 2010.
- Hamilton, J. F., Lewis, A. C., Carey, T. J., and Wenger, J. C.: Characterization of polar compounds and oligomers in secondary organic aerosol using liquid chromatography coupled to mass spectrometry, *Anal. Chem.*, 80, 474–480, 2008.
- 30 Hamilton, J. F., Webb, P. J., Lewis, A. C., and Reviejo, M. M.: Quantifying small molecules in secondary organic aerosol formed during the photo-oxidation of toluene with hydroxyl radicals, *Atmos. Environ.*, 39, 7263–7275, 2005.
- Iinuma, Y., Muller, C., Berndt, T., Boge, O., Claeys, M., and Herrmann, H.: Evidence for the ex-



**Investigating the use  
of secondary organic  
aerosol**

J. F. Hamilton et al.

Title Page

Abstract

Introduction

Conclusions

References

Tables

Figures

◀

▶

◀

▶

Back

Close

Full Screen / Esc

Printer-friendly Version

Interactive Discussion



istence of organosulfates from beta-pinene ozonolysis in ambient secondary organic aerosol, Environ. Sci. Technol., 41, 6678–6683, 2007.

Intergovernmental Panel for Climate Change: Climate Change 2007, Intergovernmental Panel for Climate Change, Cambridge University Press, Cambridge, UK, 2007.

Jang, M. S., Carroll, B., Chandramouli, B., and Kamens, R. M.: Particle growth by acid-catalyzed heterogeneous reactions of organic carbonyls on preexisting aerosols, Environ. Sci. Technol., 37, 3828–3837, 2003.

Jimenez, J. L., Canagaratna, M. R., Donahue, N. M., Prevot, A. S. H., Zhang, Q., Kroll, J. H., DeCarlo, P. F., Allan, J. D., Coe, H., Ng, N. L., Aiken, A. C., Docherty, K. S., Ulbrich, I. M., Grieshop, A. P., Robinson, A. L., Duplissy, J., Smith, J. D., Wilson, K. R., Lanz, V. A., Hueglin, C., Sun, Y. L., Tian, J., Laaksonen, A., Raatikainen, T., Rautiainen, J., Vaattovaara, P., Ehni, M., Kulmala, M., Tomlinson, J. M., Collins, D. R., Cubison, M. J., Dunlea, E. J., Huffman, J. A., Onasch, T. B., Alfarra, M. R., Williams, P. I., Bower, K., Kondo, Y., Schneider, J., Drewnick, F., Borrmann, S., Weimer, S., Demerjian, K., Salcedo, D., Cottrell, L., Griffin, R., Takami, A., Miyoshi, T., Hatakeyama, S., Shimojo, A., Sun, J. Y., Zhang, Y. M., Dzepina, K., Kimmel, J. R., Sueper, D., Jayne, J. T., Herndon, S. C., Trimborn, A. M., Williams, L. R., Wood, E. C., Middlebrook, A. M., Kolb, C. E., Baltensperger, U., and Worsnop, D. R.: Evolution of Organic Aerosols in the Atmosphere, Science, 326, 1525–1529, 2009.

Li, Y. J., Chen, Q., Guzman, M. I., Chan, C. K., and Martin, S. T.: Second-generation products of  $\beta$ -caryophyllene ozonolysis are the dominant contributors to particle mass concentration, Atmos. Chem. Phys. Discuss., 10, 17699–17726, doi:10.5194/acpd-10-17699-2010, 2010.

Liggio, J. and Li, S. M.: Organosulfate formation during the uptake of pinonaldehyde on acidic sulfate aerosols, Geophys. Res. Lett., 33, L13808, doi:10.1029/2006GL026079, 2006.

Lindinger, W., Hirber, J., and Paretzke, H.: An Ion/Molecule-Reaction Mass-Spectrometer Used for Online Trace Gas-Analysis, Int. J. Mass Spectrom., 129, 79–88, 1993.

Matsunaga, A. and Ziemann, P. J.: Gas-Wall Partitioning of Organic Compounds in a Teflon Film Chamber and Potential Effects on Reaction Product and Aerosol Yield Measurements, Aerosol Sci. Technol., 44, 881–892, 2010.

Odum, J. R., Jungkamp, T. P. W., Griffin, R. J., Forstner, H. J. L., Flagan, R. C., and Seinfeld, J. H.: Aromatics, reformulated gasoline, and atmospheric organic aerosol formation, Environ. Sci. Technol., 31, 1890–1897, 1997.

Song, C., Zaveri, R. A., Alexander, M. L., Thornton, J. A., Madronich, S., Ortega, J. V., Zelenyuk, A., Yu, X. Y., Laskin, A., and Maughan, D. A.: Effect of hydrophobic primary organic aerosols



**Investigating the use  
of secondary organic  
aerosol**

J. F. Hamilton et al.

Title Page

Abstract

Introduction

Conclusions

References

Tables

Figures

◀

▶

◀

▶

Back

Close

Full Screen / Esc

Printer-friendly Version

Interactive Discussion



on secondary organic aerosol formation from ozonolysis of alpha-pinene, *Geophys. Res. Lett.*, 34, L20803, doi:10.1029/2007GL030720, 2007.

Surratt, J. D., Kroll, J. H., Kleindienst, T. E., Edney, E. O., Claeys, M., Sorooshian, A., Ng, N. L., Offenberg, J. H., Lewandowski, M., Jaoui, M., Flagan, R. C., and Seinfeld, J. H.: Evidence for organosulfates in secondary organic aerosol, *Environ. Sci. Technol.*, 41, 517–527, 2007.

Varutbangkul, V., Brechtel, F. J., Bahreini, R., Ng, N. L., Keywood, M. D., Kroll, J. H., Flagan, R. C., Seinfeld, J. H., Lee, A., and Goldstein, A. H.: Hygroscopicity of secondary organic aerosols formed by oxidation of cycloalkenes, monoterpenes, sesquiterpenes, and related compounds, *Atmos. Chem. Phys.*, 6, 2367–2388, doi:10.5194/acp-6-2367-2006, 2006.

Volkamer, R., Ziemann, P. J., and Molina, M. J.: Secondary Organic Aerosol Formation from Acetylene (C<sub>2</sub>H<sub>2</sub>): seed effect on SOA yields due to organic photochemistry in the aerosol aqueous phase, *Atmos. Chem. Phys.*, 9, 1907–1928, doi:10.5194/acp-9-1907-2009, 2009.

Volkamer, R., Jimenez, J. L., San Martini, F., Dzepina, K., Zhang, Q., Salcedo, D., Molina, L. T., Worsnop, D. R., and Molina, M. J.: Secondary organic aerosol formation from anthropogenic air pollution: Rapid and higher than expected, *Geophys. Res. Lett.*, 33, L17811, doi:10.1029/2006GL026899, 2006.

Williams, P. I.: Construction and Validation of a DMPS for Aerosol Characterisation, PhD Thesis, University of Manchester, Manchester, UK, 1999.

Wyche, K. P., Blake, R. S., Ellis, A. M., Monks, P. S., Brauers, T., Koppmann, R., and Apel, E. C.: Technical Note: Performance of Chemical Ionization Reaction Time-of-Flight Mass Spectrometry (CIR-TOF-MS) for the measurement of atmospherically significant oxygenated volatile organic compounds, *Atmos. Chem. Phys.*, 7, 609–620, doi:10.5194/acp-7-609-2007, 2007.

Zhang, Q., Jimenez, J. L., Canagaratna, M. R., Allan, J. D., Coe, H., Ulbrich, I., Alfarra, M. R., Takami, A., Middlebrook, A. M., Sun, Y. L., Dzepina, K., Dunlea, E., Docherty, K., DeCarlo, P. F., Salcedo, D., Onasch, T., Jayne, J. T., Miyoshi, T., Shimonono, A., Hatakeyama, S., Takegawa, N., Kondo, Y., Schneider, J., Drewnick, F., Borrmann, S., Weimer, S., Demerjian, K., Williams, P., Bower, K., Bahreini, R., Cottrell, L., Griffin, R. J., Rautiainen, J., Sun, J. Y., Zhang, Y. M., and Worsnop, D. R.: Ubiquity and dominance of oxygenated species in organic aerosols in anthropogenically-influenced Northern Hemisphere midlatitudes, *Geophys. Res. Lett.*, 34, L13801, doi:10.1029/2007GL029979, 2007.

## Investigating the use of secondary organic aerosol

J. F. Hamilton et al.

**Table 1.** Experimental details and SOA yields.

Experiment Date	Phase 1 $[\text{VOC}_{\beta-c}]_0^a$ /ppbV	Phase 2 $[\text{VOC}_{\text{lim}}]_0^a$ /ppbV	$\Delta[\text{VOC}_{\beta-c}]$ /ppbV	$\Delta[\text{VOC}_{\text{lim}}]$ /ppbV	Phase 1 $\text{VOC}/\text{NO}_x^a$	Phase 3 $\text{VOC}/\text{NO}_x^a$	Phase 1 Peak Seed SOA mass <sup>b</sup> / $\mu\text{gm}^{-3}$	Phase 3 Peak Measured SOA mass <sup>c</sup> / $\mu\text{gm}^{-3}$	Phase 3 Peak Condensed SOA mass <sup>d</sup> / $\mu\text{gm}^{-3}$	$Y_{\text{SOA}}$ Phase 1 (Seed) /%	$Y_{\text{SOA}}$ Phase 3 (Condensation) <sup>e</sup> /%
25/06/08	48.77 ( $\pm 8.71$ )	92.82 ( $\pm 10.19$ )	44.80	85.39	1.42	2.00	35.58	69.60	65.33	9.52	13.75
26/06/08	52.35 ( $\pm 9.26$ )	20.83 ( $\pm 3.58$ )	40.78	20.24	1.88	1.31	53.21	13.46	6.93	15.64	6.15
10/07/08	48.10 ( $\pm 8.60$ )	52.61 ( $\pm 6.69$ )	41.84	48.39	0.64	1.88	65.80	44.76	31.28	18.86	11.62

<sup>a</sup>  $[\text{VOC}]_0$  and  $\text{VOC}/\text{NO}_x$  based on 5 min integrated CIR-TOF-MS and  $\text{NO}_x$  data, <sup>b</sup> Maximum measured SOA mass during Phase 1 of the experiment, <sup>c</sup> Maximum measured SOA mass during Phase 3 of the experiment, <sup>d</sup> Maximum SOA formed from condensation during Phase 3, <sup>e</sup> SOA yield from condensation during Phase 3

[Title Page](#)
[Abstract](#)
[Introduction](#)
[Conclusions](#)
[References](#)
[Tables](#)
[Figures](#)
[Back](#)
[Close](#)
[Full Screen / Esc](#)
[Printer-friendly Version](#)
[Interactive Discussion](#)


## Investigating the use of secondary organic aerosol

J. F. Hamilton et al.

Title Page

Abstract

Introduction

Conclusions

References

Tables

Figures

◀

▶

◀

▶

Back

Close

Full Screen / Esc

Printer-friendly Version

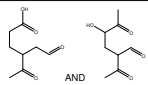
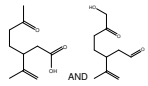
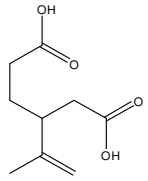
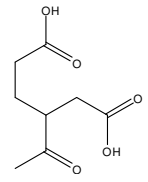
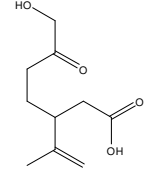
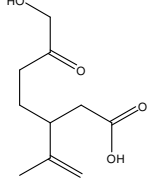
Interactive Discussion



**Table 2.** Limonene oxidation products identified in seeded SOA.

Mass of product	[M+Na] <sup>+</sup>	Potential molecular formula	Identified products
116	139	C <sub>5</sub> H <sub>8</sub> O <sub>3</sub> C <sub>6</sub> H <sub>12</sub> O <sub>2</sub>	
154	177	C <sub>9</sub> H <sub>14</sub> O <sub>2</sub>	
156	179	C <sub>9</sub> H <sub>16</sub> O <sub>2</sub> C <sub>8</sub> H <sub>12</sub> O <sub>3</sub>	
168	191	C <sub>10</sub> H <sub>16</sub> O <sub>2</sub>	
170	193	C <sub>9</sub> H <sub>14</sub> O <sub>3</sub>	

**Table 2.** Continued.

Mass of product	[M+Na] <sup>+</sup>	Potential molecular formula	Identified products
172	195	C <sub>8</sub> H <sub>12</sub> O <sub>4</sub>	
184	207	C <sub>10</sub> H <sub>16</sub> O <sub>3</sub>	
186	209	C <sub>9</sub> H <sub>14</sub> O <sub>4</sub>	
188	211	C <sub>8</sub> H <sub>12</sub> O <sub>5</sub>	
200	223	C <sub>10</sub> H <sub>16</sub> O <sub>4</sub>	
216	239	C <sub>10</sub> H <sub>16</sub> O <sub>5</sub> C <sub>9</sub> H <sub>12</sub> O <sub>6</sub>	

25144

**Investigating the use of secondary organic aerosol**

J. F. Hamilton et al.

Title Page

Abstract

Introduction

Conclusions

References

Tables

Figures



Back

Close

Full Screen / Esc

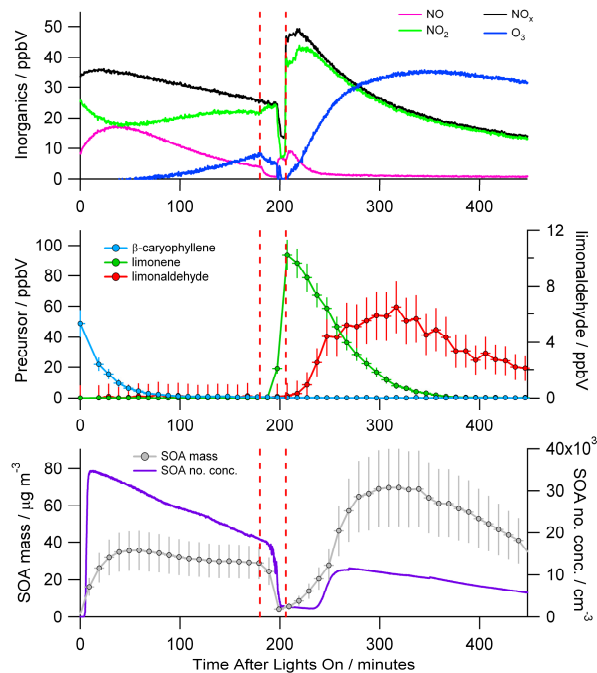
Printer-friendly Version

Interactive Discussion



**Investigating the use  
of secondary organic  
aerosol**

J. F. Hamilton et al.

**Fig. 1.** Evolution of basic chamber measurements during 25 June 2008 experiment.

Title Page

Abstract

Introduction

Conclusions

References

Tables

Figures

◀

▶

◀

▶

Back

Close

Full Screen / Esc

Printer-friendly Version

Interactive Discussion



## Investigating the use of secondary organic aerosol

J. F. Hamilton et al.

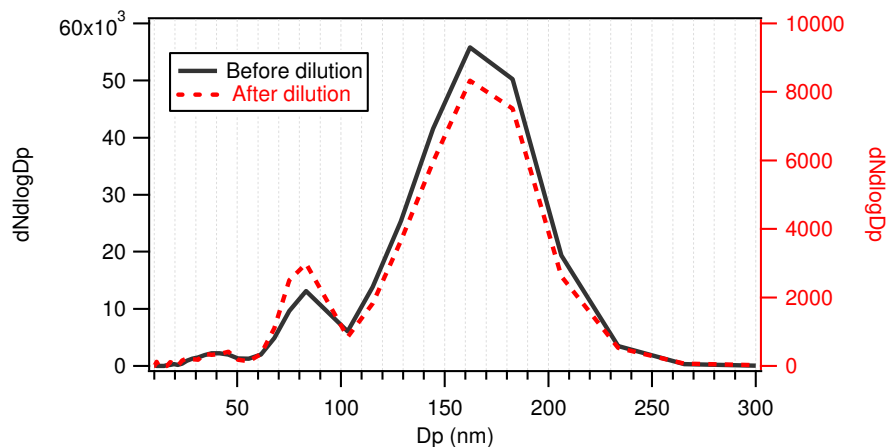


**Fig. 2.** Particle size distribution of the  $\beta$ -caryophyllene seed particles. Black line indicates size distribution at the end of Phase 1 (pre-dilution). Red line indicates size distribution at the end of Phase 2 (after flushing and dilution).

[Title Page](#)[Abstract](#)[Introduction](#)[Conclusions](#)[References](#)[Tables](#)[Figures](#)[◀](#)[▶](#)[◀](#)[▶](#)[Back](#)[Close](#)[Full Screen / Esc](#)[Printer-friendly Version](#)[Interactive Discussion](#)

## Investigating the use of secondary organic aerosol

J. F. Hamilton et al.

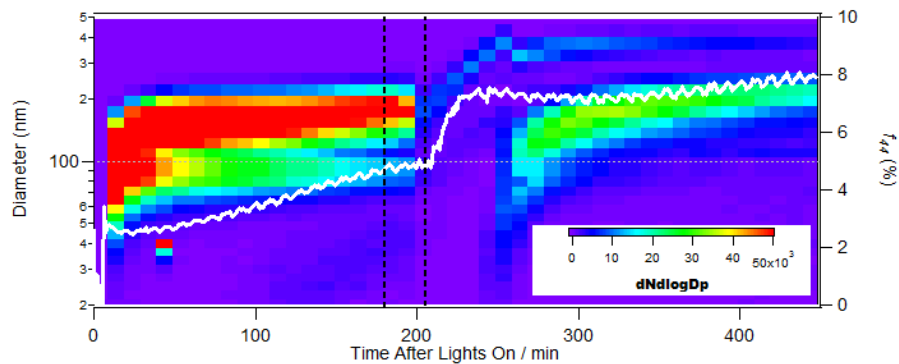


**Fig. 3.** Particle size distribution during 25 June 2008 experiment and  $f_{44}$ (%) from the AMS measurements.

[Title Page](#)[Abstract](#)[Introduction](#)[Conclusions](#)[References](#)[Tables](#)[Figures](#)[◀](#)[▶](#)[◀](#)[▶](#)[Back](#)[Close](#)[Full Screen / Esc](#)[Printer-friendly Version](#)[Interactive Discussion](#)

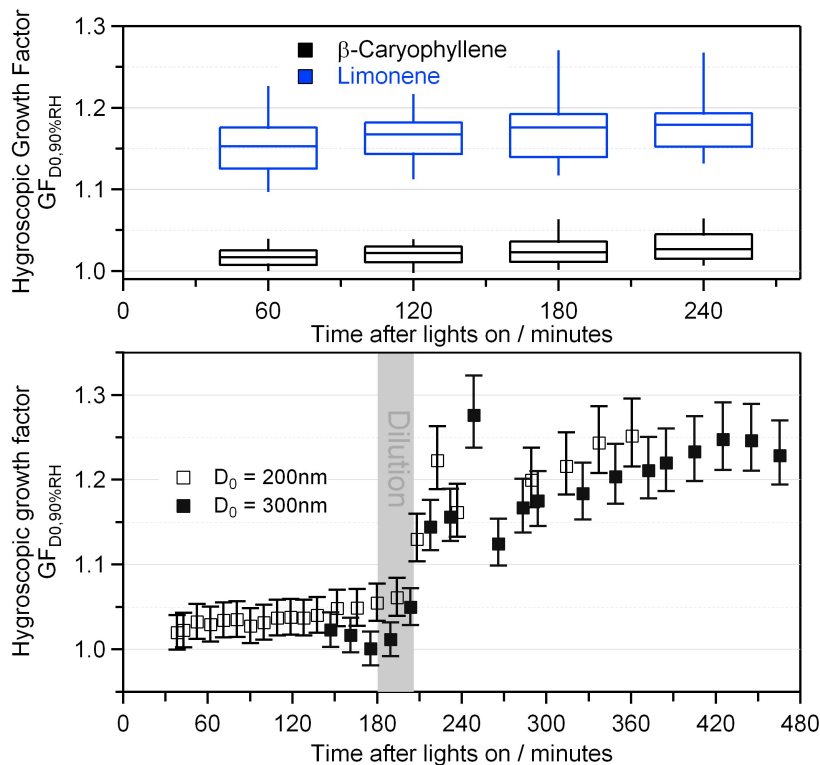


**Fig. 4.** Hygroscopic growth factor measurements at 90%RH. The upper panel shows the growth factors of un-seeded limonene and  $\beta$ -caryophyllene experiments. The data is averaged over 60 min intervals, box (25-th and 75-th percentile) and whisker (5-th and 95-th percentile) plots show the range of pure precursor growth factors measured. The lower panel shows the evolution of the growth factor with time of the  $\beta$ -caryophyllene seed aerosol which is diluted (after 180 min) to act as seed for the subsequent limonene injection (at 205 min).



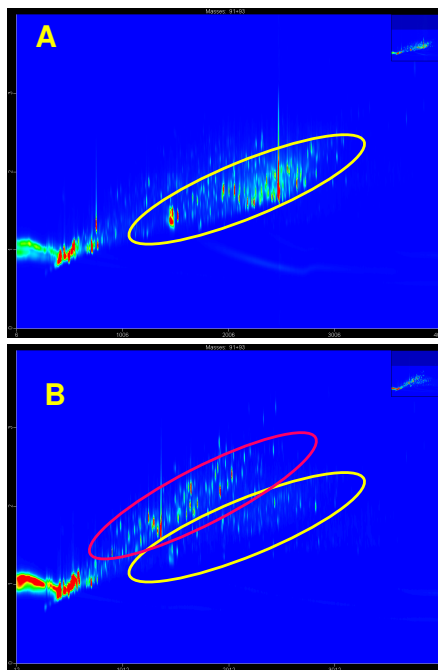


**Fig. 5.** GCxGC extracted ion contour plots ( $m/z93 + 91$ ) – **(A)**  $\beta$ -caryophyllene seed. **(B)** Limonene SOA + seed. Yellow circle indicates highest concentration of seed compounds. Pink circle indicates limonene SOA compounds.

**Investigating the use of secondary organic aerosol**

J. F. Hamilton et al.

Title Page	
Abstract	Introduction
Conclusions	References
Tables	Figures
◀	▶
◀	▶
Back	Close
Full Screen / Esc	
Printer-friendly Version	
Interactive Discussion	



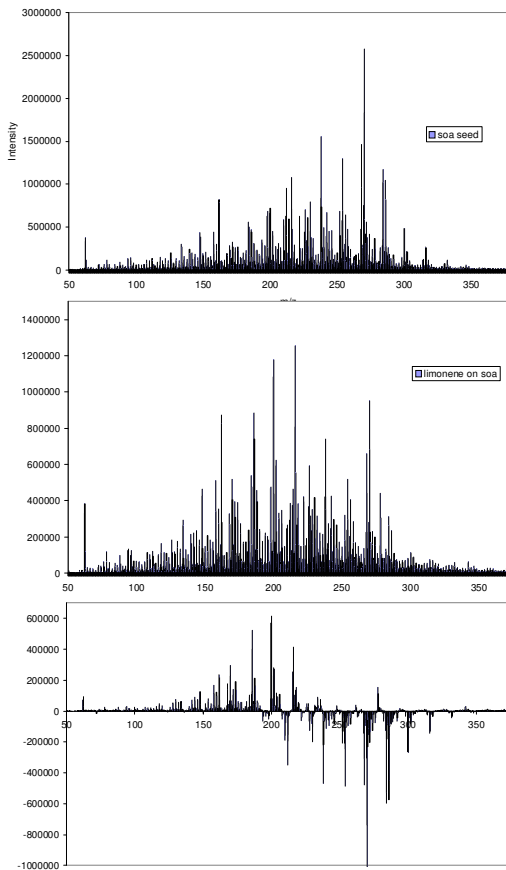


**Fig. 6.** Average mass spectrum of filter extracts. Upper:  $\beta$ -caryophyllene seed. Middle: limonene SOA + seed. Lower: difference mass spectra.

**Investigating the use of secondary organic aerosol**

J. F. Hamilton et al.

Title Page

Abstract Introduction

Conclusions References

Tables Figures

◀ ▶

◀ ▶

Back Close

Full Screen / Esc

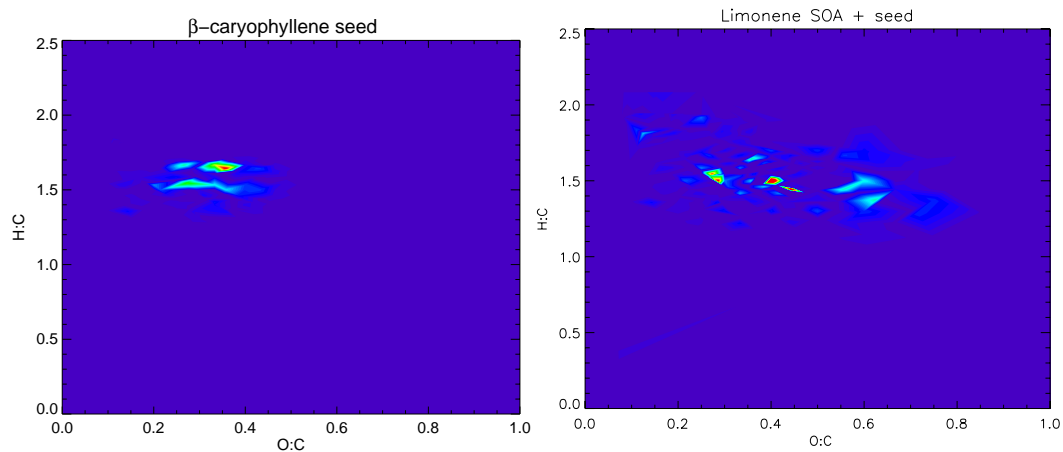
Printer-friendly Version

Interactive Discussion



**Investigating the use  
of secondary organic  
aerosol**

J. F. Hamilton et al.

**Fig. 7.** 3-D Van Krevelen diagrams for the seed and limonene SOA + seed.

Title Page

Abstract

Introduction

Conclusions

References

Tables

Figures

◀

▶

◀

▶

Back

Close

Full Screen / Esc

Printer-friendly Version

Interactive Discussion

